SDPD simulation of spider silk formation

Sergey Litvinov

Computational Science and Engineering Laboratory, ETH Zurich, Switzerland

2018

1 Summary

Natural silk has a combination of strength and extensibility which is out of reach for synthetic materials. These properties are attributed to the structure of the silk. It has several levels: amino acids form protein chains, which are organized in co-existing phases: beta-sheet nanocristalls (responsible for strength) and a semi-amorphous matrix of glycine-rich repeats (responsible for extensibility). To understand this material it is natural to use multi-scale or mesoscale simulation methods.

Recently such approaches were very successful in establishing the link between molecular-level effects and macroscopic properties of the silk [1], but as it was emphasized in review article [2] there is a lack of modeling works which take into account silk processing conditions.

During spinning silk undergoes a transformation from highly concentrated liquid media to strong almost dry fibers. This transformation is accompanied by a change in water concentration, salt concentration, the material experiences mechanical forces caused by shear and extensions. How those processes affect fiber formation is not understood. Despite being one of the most studied subjects in bio-material sciences the spinning process still cannot be reproduced ex vivo.

Spiders do not just produce material with superior characteristics but it is done in a surprisingly efficient way [3] . The spider manages the production under very mild conditions: room temperature, close to neutral pH, no extreme mechanical loading. Natural spinning is also very robust: highly concentrated protein solutions tend to crystallize, and if this process occurs prematurely in the spinning organ it would be difficult for the animal to pull out the dry silk. However, the timing of the process is such that solidification of the fibers is completed just before leaving the organ.

Furthermore, the synergistic nature of the fiber formation is still to be uncovered. Taken apart, the physical, chemical, and mechanical processes involved in spinning are well studied and allow atomistic and mesoscale modeling. We propose to model spider silk spinning in vivo by Smoothed Dissipative Particle Dynamics (SDPD). With this method solvent and proteins are represented as particles interacting with each other. SDPD correctly represents hydrodynamic interactions, the wall built from SDPD particles is impenetrable for fluid particles making it straightforward to model complex geometries.

SDPD is sharing some important properties of traditional coarse-grained methods. The properties of the chain beads will be manipulated to represent atomistic level phenomena such as effect of the salt concentration, effect of pH, micelles formation. We believe that such a mesoscale model can be a valuable tool to test hypotheses about silk spinning by computer simulation.

2 State of the Art

2.1 Introduction

In this section we briefly outline the anatomy of the spider silk spinning organs and introduce some terminology. The only visible part of the spinning organs is *the spinneret* a small tube-like structure on the

underside of the spider. Most of the species have several of such structures and each spinneret has a gland which supplies almost ready silk.

In Figure 1 the gland of the *Nephila clavipes* (a species of golden orb-web spider) is shown. The *Tail* is a part of the gland where the spider secretes proteins. In the *Ampulla* the concentrated protein solution is stored. This solution is called *spinning dope*. The *Funnel* is a narrowing transition region from the Ampulla to the *Duct* (blue color in the photo). The Duct consists of several *Limbs* and ends with the *Valve* and the *Spigot*. Limbs and possibly the valve is where protein dope undergoes interconnected chemical, physical and rheological transformations and turns into solid silk material. The timing of the silk formation process is exactly controlled, the spider avoids the spreading of the assembly process to the ampulla.

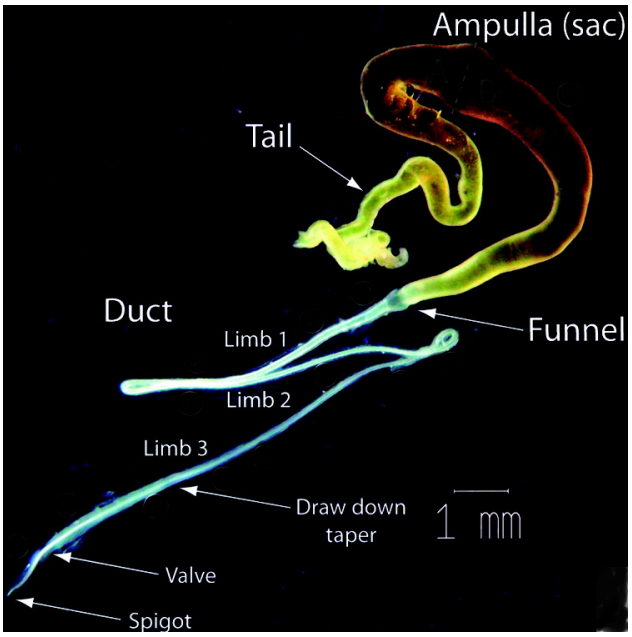

Figure 1: *N. clavipes* gland [4]. The Duct is shown in blue.

Figure 2 shows a schematic of a silk fiber: solid noncrystalline β-sheets are immersed in a semi-amorphous matrix. Although individual hydrogen bonds are relatively weak the high density of such bonds inside β-sheets makes it strong. Both amorphous and crystallized phases are made of interconnected protein chains. The link between microstructure and the exceptional mechanical properties of the silk fibers is an area of intensive research, in particular a recent survey of multiscale studies is given in reference [1].

2.2 Spidroins

The type of proteins that make the major part of the silk fibers are called *spidroins*. They are relatively big ($> 30\,000$ amino acids) in comparison with others proteins. Spidroins (see Figure 3) are block co-polymers containing stretches of poly-alanine (hydrophobic) and glutamine and glycine-rich elements (hydrophilic) as a core, flanked by non-repetitive N- and C- terminals. For meso-scale modeling it is important to note that a glycine block is the simplest amino acid and it makes the chain very flexible [6]. Recently NMR data [7] helped to solve the structure of the terminal domains [8, 9]. Some models suggest the crucial role of the terminal domains in spinning.

The concentration of spidroin proteins in the ampulla can be as high as 50 wt %. For such concentration the solutions of proteins tend to irreversibly aggregate, and it is unusual that the spinning dope can be stored in liquid form for several days. Dope is a highly non-Newtonian fluid with extensional viscosities increasing 100-fold with applied strain. The shear viscosity of the dope is best described by the phenomenological Carreau-Yasuda constitutive model [11]. This relation is characteristic for the polymer melts, also silkworm silk dope shows remarkable similarity to spider dope. Holland and co-authors write: *"Surprisingly, [spider*

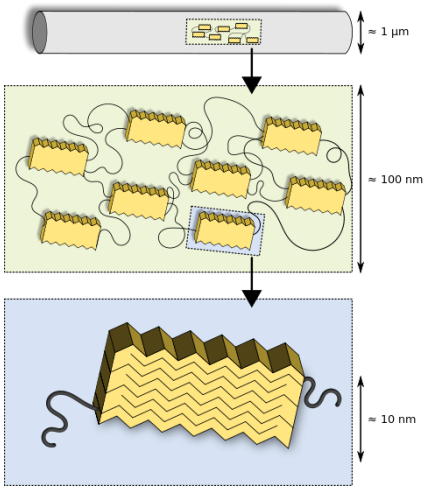

Figure 2: Structure of spider silk [5].

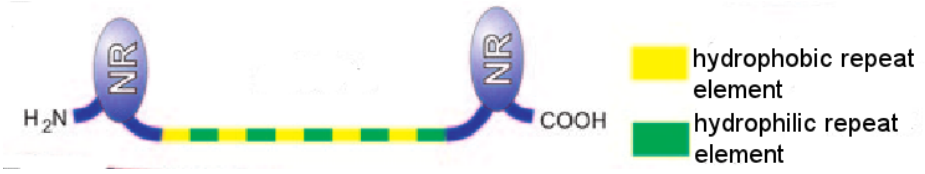

Figure 3: Spidroin consists of hydrophobic polyalanine-rich motif, hydrophilic glutamine and glycine-rich motif, C- and N- terminal domains (figure is from [10])

and silkworm] dopes behave like typical polymer melts. This observation opens the door to using polymer theory to clarify our general understanding of natural silks" [12].

Concerning the conformation of the spidroins in the ampulla there are several opinions in the literature. Vollrath and Knight found that spidroins adopt a liquid-crystalline phase, with the molecules oriented parallel to each other and perpendicular to the secreting epithelium [13]. According to Jin and Kaplan [14] and Hagn and co-workers [9] proteins form spherical (globule-like) micelles with terminal domains on the surface of the structure [15] and hydrophilic parts inside. This model does not exclude the existence of the liquid-crystalline phase which may form prior to or concurrently with the micelles. Although recent high-resolution magic angle spinning experiments [16] indicate a random coil structure, this result can be consistent with the micelles model because the method targets mostly the repetitive region of the proteins and structures involving terminal domains are not detected.

2.3 Passage through the spinning duct

After passage through the spinning duct the spidroins turn into solid fibers. This transformation is accompanied by shear and extensional flow and changes in the content of the solution: increase in potassium and phosphate concentration, a decrease in sodium and chloride concentration, removal of water, and acidification [9]. In the following we outline what is known about these factors.

2.3.1 Channel geometry

The shape of the *Nephila* MA gland was reported by Knight et al. [17] and confirmed by independent measurements [18]. Breslauer et al.[19] fitted the radii (r) of the gland as a function of axial position (z) with a two-stage exponential function:

$$r(z) = ae^{bz} + ce^{dz}, \tag{1}$$

Similar hyperbolically shaped funnels are used in industrial-fiber spinning [19]. This shape leads to approximately linear increase in shear rate with the position along the gland. Note that this geometry neglects the folding of the gland. It is normally has an “S-shape” and it may influence the flow structure.

The shape of the gland influences the orientation of molecules and recent data of *in vivo* Raman spectromicroscopy (see Figure 4) give the following picture. The proteins in spinning dope are initially isotropic and remain isotropic up to the second limb where the first β-sheets start to develop under the influence of shear forces. These β-sheets serve as nucleation sites. Alignment of the polypeptide chains occurs near the valve. This suggests that extensional flow is the driving force to produce the chain orientations [20].

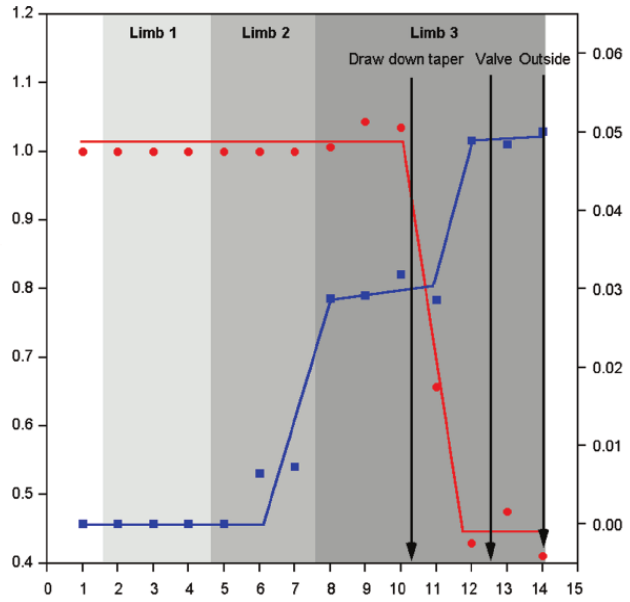

Figure 4: Conformation (blue) and orientation (red) of silk proteins. Qualitative characteristics based on Raman spectromicroscopy data [4].

2.3.2 Water concentration

In [21] the water content of the silk produced by the spider *Argiope auranti* was compared to the content of major ampullate. It was found that the ampullate content is around $50\,\%$ of water, and silk fibers are dry. Kojic and co-authors [18] by combination of ex vivo experiments and numerical modeling obtained the water diffusion coefficient of the dope for one species of golden orb-web spider – *N*ephila Clavipes. The coefficient does not depend on protein concentration. In contrast, for synthetic solutions out of which fibers are spun the diffusion coefficient decreases with the increasing of protein concentration. Assuming that diffusion of water through the dope is a rate limiting step in water removal and that the water concentration tends to zero, simple numerical models give an estimation of the required spinning velocity which is in good agreement with experimental results. Possibly specialized epithelial cells on the surface act as water pumps and are responsible for the quick water removal [13].

2.3.3 Salt concentration

In the ampulla spidroins are stored in the presence of sodium (Na^-) and chloride ions (Cl^-). During spinning these ions are exchanged for potassium (K^+), phosphate (P), and sulfur (S) [22]. For *Argiope auranti* the ratio of K^+/Na^+ is changing from 0.6 to 2.4 during spinning [21].

The mechanism of salt regulation and effect of salt concentration on the spinning process is not fully understood. Ex vivo experiments show that chloride does not cause protein aggregation, while the presence of phosphate leads to significant levels of protein aggregation [23]. Studies of spidroin films and show that

increase of KCl concentration changes qualitatively the conformation transition of the protein, this effect can be explained by weakening of hydrogen bonds [24].

2.4 Models of the silk spinning

There are two qualitative models of the spinning process: one involving micelles formation and another involving liquid crystal phase. We believe that these models do not exclude each other: both assume some kind of protein chain arrangement which prevent the premature formation of β-sheets, and this barrier can be broken by solvent removal or by flow.

2.4.1 "Micelles" model

This model relies on the microstructure of the individual protein molecule. Spider silk proteins are stored at neutral pH and high sodium chloride concentration. To prevent proteins from crystallization the following mechanism is used: proteins adopt a micelle configuration with hydrophilic terminal domains outside and hydrophobic repetitive core inside the micelle [9, 14] (see top of Figure 5).

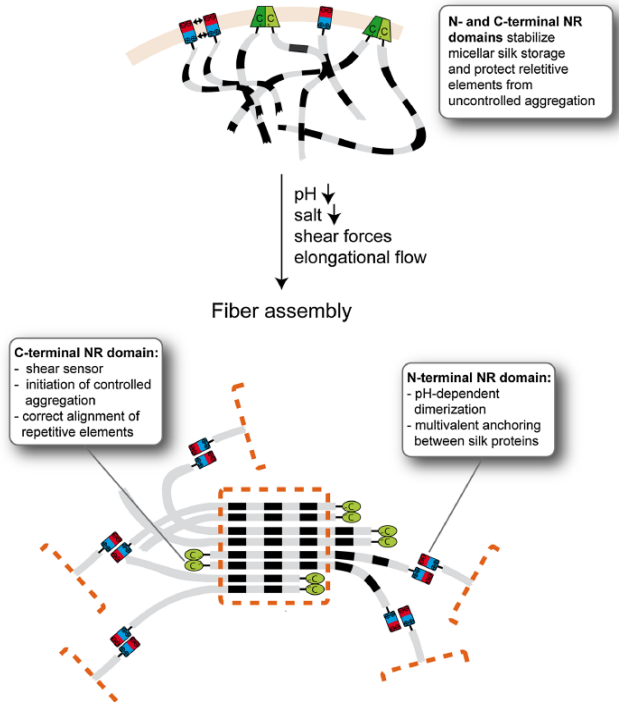

Figure 5: In the ampulla terminal domains are on the the surface of micelles. During spinning the N-terminal domain serves as a pH-dependent anchoring between silk proteins (note that the orientation of the dimers in N-terminal domain sites is changing from parallel to antiparallel, this leads to the long chains of the proteins) [9].

During the spinning process pH and ionic concentration are changing and N-terminal domains tend to demirize. C-terminal domains are sensitive to shear and elongation forces and act as anchoring points for the precise alignment of the molecules [8]. Also the orientation of the dimers at N-terminal domains sites is changing from parallel (favors compact formations) to anti-parallel (favors long chain formations). The structure of the silk is finalized by the development of β-sheets. (see bottom of Figure 5).

2.4.2 "Liquid crystal" model

Several models were proposed to explain unique properties of the dope with reference to how relative configuration of proteins is changing during the spinning. According to Vollrath and co-workers [6, 13] proteins adopt a "string-of-beads" structure where each "bead" has about 7 folds of 10–12 peptide segments (see Figure 6). "Beads" are the building blocks of the nematic liquid crystal phase.

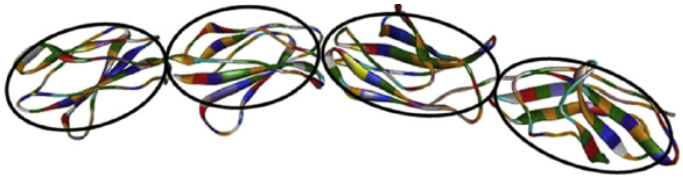

Figure 6: "String of beads" structural element [6]

Figure 7 shows the morphology development of the dope under shear and extensional flow: "beads" are aligned into "strings", but this transition does not lead to the alignment of the individual chain along the axis. Note that this model assumes only moderate changes of the chain configuration in the gland: the final morphology is predefined in the ampulla.

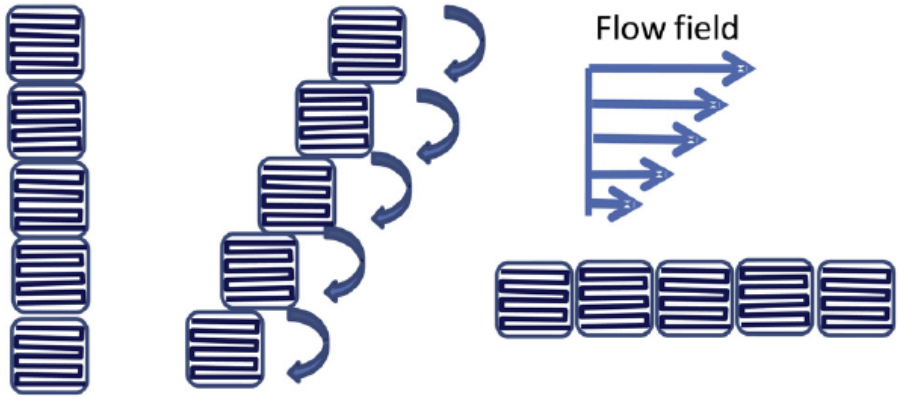

Figure 7: Schematic suggestion of morphology development from stored protein feedstock to final fibres under shear flow. [13]

This model is supported by the recent Rheo-IR experiments [25]. This technique combines infrared spectroscopy and rheological measurements. Infrared spectroscopy can probe the molecular orientation of any polymer melt and it was shown that shear thinning of the dope is caused by molecular alignment, and is associated with the onset of a rapid solidification promoted by β-sheet formation.

Rey and Herrera-Valencia [26] derived spinning models as applications of general theories of liquid crystals (Leslie Erciksen model and Landau-de Gennes viscoelastic models). Those models explain the following experimental observations: (i) tactoidal states, (ii) chiral textures, and (iii) defect lattice textures along the duct of silkworms and spiders.

Moreover, recently it was proposed that the dope in the Ampulla is in a unique state of matter called "aquamelt" [3]. Solidification of the "aquamelt" can be achieved in very efficient way (it needs 1000 times less energy than for typical polymers) due to interactions between proteins and its bonded water.

Major evidence for the existence of "aquamelt" are:

- The viscosity of the natural silk solution is 5 orders of magnitude larger than that of re-constituted silk [27];
- for natural silk the viscosity is proportional to the second power of the concentration instead of the expected power 5 dependence [27];

- fibrillation in silk is driven by shear rate [3], in the synthetic polymer it is driven by strain;
- energy cost of solidification for natural silk is very low and independent on the environment conditions.

Although recently quantum dynamics simulation were used to understand bonded water-protein interactions [28] in [6] authors suggested that meso-scale analysis still is necessary: *"a theoretical analysis of the rheological properties of such a solution that includes inter- chain and inter-string hydrogen bonding would be very useful and also be self-consistent with polymer science concepts."*

2.5 Finite element method (FEM) simulations

The two models we have outlined in the previous section are detailed and supported by experimental measurements but were not presented in the form which allows for quantitative predictions. However, several groups have performed FEM simulation of the spinning process.

Moriya and co-authors reported FEM simulation with geometries for two species of silkworms (*Bombyx mori* and *Samia cynthia ricini*) [29, 30]. The following assumtions were made: temperature is constant; liquid is viscous with shear dependent viscosity; no slip boundary condition at the wall; pH, ionic concentration, and water content are constant. Critical shear rate was used as criterion for the crystallization, and two sets of parameters describe the viscosity of the liquid and the crystallized phase:

$$\eta = a_1 \dot{\gamma}^{n_1}, \quad \dot{\gamma} \leq \dot{\gamma}_c, \tag{2}$$

$$\eta = a_2 \dot{\gamma}^{n_2}, \quad \dot{\gamma} > \dot{\gamma}_c, \tag{3}$$

where $\dot{\gamma}$ is the shear rate, $\dot{\gamma}_c$ is the critical shear rate for crystallization, $n_{1,2}$ and $a_{1,2}$ are two sets of fitting parameters for the material before and after crystallization.

The simulation results indicate the place in the flow channel where crystallization starts and suggest that shear rate plays a dominant role in the crystallization process. However, the extrusion pressures in the simulations and in the experiment are different. This difference suggests that some rheologically important phenomena are missing from the model.

Another FEM simulation of the spider and silkworm glands were performed by Breslauer and co-authors [19]. The non-Newtonian viscosity of the liquid was described by the Carreau-Yasuda model

$$\eta = \eta_0 \left((1 + \dot{\gamma}\lambda)^a\right)^{(n-1)/a}, \tag{4}$$

where $\dot{\gamma}$ is shear rate, η_0 is zero shear rate viscosity, λ is a relaxation time of the fluid, a is the rate of transition from zero-shear viscosity to shear-thinning behavior, n is the exponent characterizing the shear-thinning. No-slip boundary conditions were used. The simulations show qualitative differences between flows in the spider and silkworm silk glands. But again a significant mismatch between experimental integral flow parameters and simulation results (outlet velocities, residence time) is reported.

Despite producing valuable insights the macroscale simulation of spider and silkworm gland are currently suffering from the inability of the governing equations to describe the behavior of the dope. The authors [19, 30] express their hope that the predictive capability of macroscale simulations can be improved by incorporating more detailed physical processes and possibly molecular-level phenomenon. Breslauer and co-authors write: *"Until studies are available that correlate the molecular alignment, structure, and rheological behavior (i.e., that specify the values of the multiple material constants in the Leslie-Ericksen theory), we are limited to simplified models of the flow of silk secretions"*

Moreover a recent review on structure-process-property relationships in biopolymer [2] concerning modeling of silk states: *"processing conditions [of silk] have not yet been taken into account for silk by modeling, despite the fact that experimental investigations show a significant dependence on parameters such as pH, ion concentration and shear forces"*.

3 Objectives

The main objective of the work is to understand the process of spider silk spinning *in vivo*. We will trace an individual protein from the Ampulla to the spigot and relate its transformations to the macroscopic properties

of the media. We are planning to have a model of spider silk spinning process “in silica” with the ultimate goal to enhance our assist in the improvement of industrial spinning process.

- A summary of experimental data and simulations results in written form. It can be slightly more extended than typical “Introduction” section of a scientific article
- A computational model of spider silk formation which includes mobility of water, pH and salt effects and effect of the flow field on the material
- An parallel implementation of the computational model in an open-source software package LAMMPS [31]
- Results of the simulations help establish a link between geometry of the gland and the characteristics of the fibers

4 Plan

4.1 Preparatory work

As a first step of the project we **collect and summarize experimental data on spider silk spinning**. We already identified several recent review articles [1, 9, 32] and found that there are competing theories of spinning and it is important to understand what experimental evidence (rheological measurements, spectroscopy, composition of the dope) support each of the theories and how this data can serve as benchmarks for mesoscale simulations.

We plan to include into the model the formation of micelles and β-sheets. For example, a series of papers by Schor and co-authors on simulations of β-sheets and fiber formation by coarse-grained molecular dynamics [33–35] can provide valuable input for the mesoscale model. Another starting point is reference [36] where authors simulated micelle formation [14] using a DPD model with chains of hydrophobic and hydrophilic beads. Although the comprehensive model of micelles formation in the spinning dope is still to be developed DPD models proved to be useful for related systems: micellization-demicellization processes and micellar shuttle of diblock copolymer in a water/ionic-liquid [37], and enzymatic polymerization of DNA amphiphile into star-like micelles [38]. A more generic study of diblock co-polymer micellization was done by Li and Dormidontova [39], they found that the micelle structure in simulations is in good agreement with experimental data.

4.2 Method Development

We will use a relatively new type of DPD method, called smoothed dissipative particle hydrodynamics (SDPD). It was used to investigate the static and dynamic behaviors of the polymers [40–42]. Being the mesoscopic extension of a popular particle-based method applied to continuum flow, e.g. smoothed particle hydrodynamics (SPH) [43], SDPD allows for an arbitrary equation of state and to specify transport coefficients directly [44, 45].

The equation of motion of one SDPD particle is

$$m_i \frac{dv_i}{dt} = \sum_j \mathbf{F}_{ij}^C + \mathbf{F}_{ij}^D + \mathbf{F}_{ij}^R \tag{5}$$

where m_i is mass of the particle, $\mathbf{F}_{ij}^{\{C,D,R\}}$ are conservative, dissipative, and random force acting on particle i from particle j. All forces $\mathbf{F}_{ij}$ depend on position and velocity of particles i and j, and also include density which is defined as

$$\rho_i = \sum_j m_j W(\mathbf{x} - \mathbf{x}_j) \tag{6}$$

where $W(\mathbf{r})$ is a smoothing kernel.. The inclusion of density is an extension over other particle methods. The SDPD form of the conservative force precludes penetration of walls by fluid particles [46].

In the original SDPD model of polymers [47] the solvent particles fully consist of water and polymer beads contain mostly water with some fraction of atoms belonging to the polymer chain. In our preliminary simulations for this project we found that the solvent-particle diffusion coefficient does not depend on the concentration of the polymer. This is in agreement with experimental findings for spidroins [18], but for highly concentrated solution of casein (another type of protein) the NMR measurements show a strong dependency of the diffusion coefficient on protein concentration [48]. It is relatively straightforward to **model the mobility of the water which belongs to the polymer beads**. It can be done by adjusting parameters of bead-bead and bead-solvent interactions.

As a building block for **a pH and salt concentration model** we consider DPD simulations presented by Vishnyakov and co-authors [49]. This model uses a Morse potential with varying parameters to represent effects of hydrogen bonding and charge on polymer beads to represent effects of pH. We plan **to transfer this approach to SDPD**. We expect that in SDPD it is possible to avoid some complexity in implementation of electrostatic interaction over DPD [50]. Due to stronger repulsive interaction between particles one can directly calculate the force between charged particles and avoid intermediate projection of the potential field to the grid.

We plan **to model the role of terminal domains**. For N-terminal domains an increase of pH triggers dimerization, C-terminal domains are sensitive to shear and elongation forces and act as anchoring point in alignment of the chains. We believe a model with specialized function of the end beads of the chains can serve as a first approximation of this behavior.

A model of liquid crystal phase. Existing models of the spinning dope are macroscopic [19, 29, 30] with change of the rheology of the dope during spinning represented by parameters in the constitutive relation. Incorporating of even simple molecular-level features can be an improvement (although with increasing computational effort).

SDPD model of polymer melt is a good starting point for building such a better model of the dope: many authors noted remarkable similarity of rheology of dopes and polymer melts [12], in out previous work we found that DPD or SDPD model of polymer melt follows the same constitutive relation as the dope (Carreau-Yasuda model) [51, 52]. To justify the choice of SDPD as a simulation method we would like to point to the successful applications of particles based method to modeling of phase transaction of nematic liquid crystal [53]. Similar methods are used to simulate nanoparticle self-assembly in polymeric systems: see [54] for a comprehensive review and [55] for an example of the simulation involving shear-induced reorientations and phase transitions.

The important benchmark for the success of the modeling are the characteristics of the resulting fibers. Given that the structure of the dry silk is not fully understood and is subject of complex modeling work, we will not aim at a detailed but rather a suitably coarse-grained model of **the fibers "in silica"**. Instead properties of the material can serve as benchmarks and optimization targets. For example, empirical model which defines structure in terms of "ordered" and "disordered" fractions of peptide segments, without going into details of specific space groups, is very successful in predicting mechanical properties of the silk and gives the typical values of ordered fraction [56, 57]. Consequently, the values of "ordered" fraction can be used as a benchmark.

Some parameters of the spinning are known and can be used for validation such as spinning speed, tension, and pressure drop, rate of water removal [18, 58]. Low energetic cost is a distinct feature of natural spinning [3]. Hence the configuration of "in silica" spinning process should be energy-optimal within certain range of modeling conditions. Further data for comparison can be deduced from evolutionary [59] and individual [60] development of the silk producing species.

4.3 Simulations and analysis of the results

At this stage we plan to have a model of spider silk spinning process "in silica". Such a model will involve many assumptions but those assumptions will be explicitly stated, and the effect of all conditions can be directly tested in the simulations. To estimate the computational effort required to perform a full simulation we looked at representative works using similar approaches: in a study involving micelles self-assembly [61] the authors used $192\,000$ particles and in a study involving rigid-chain polymer liquid crystal [62] a typical simulation was with $81\,000$ particles. Although we plan to use a model which is more complex even a tenfold increase in number of discretization elements is feasible ($< 10\,000\,000$ particles).

We expect that the simulations will contain information on the flow field, composition and microstructure of the dope. Analysis of the simulation result can help to establish a link between geometry of the gland and the characteristics of the fibers.

References

1. Tarakanova, A. & Buehler, M. J. A Materiomics Approach to Spider Silk: Protein Molecules to Webs. *JOM* **64,** 214–225 (2012).
2. Gronau, G., Krishnaji, S. T., Kinahan, M. E., Giesa, T., Wong, J. Y., Kaplan, D. L. & Buehler, M. J. A review of combined experimental and computational procedures for assessing biopolymer structure-processproperty relationships. *Biomaterials* **33,** 8240–8255 (2012).
3. Holland, C., Vollrath, F., Ryan, A. J. & Mykhaylyk, O. O. Silk and Synthetic Polymers: Reconciling 100 Degrees of Separation. *Advanced Materials* **24,** 105109 (2012).
4. Lefevre, T., Boudreault, S., Cloutier, C. & Pezolet, M. Conformational and Orientational Transformation of Silk Proteins in the Major Ampullate Gland of Nephila clavipes Spiders. *Biomacromolecules* **9,** 2399–2407 (2008).
5. Nova, A., Keten, S., Pugno, N. M., Redaelli, A. & Buehler, M. J. Molecular and Nanostructural Mechanisms of Deformation, Strength and Toughness of Spider Silk Fibrils. *Nano Letters* **10,** 2626–2634 (2010).
6. Vollrath, F. & Porter, D. Silks as ancient models for modern polymers. *Polymer* **50,** 5623–5632 (2009).
7. Lin, Z., Huang, W., Zhang, J., Fan, J.-S. & Yang, D. Solution structure of eggcase silk protein and its implications for silk fiber formation. *Proceedings of the National Academy of Sciences* **106,** 8906–8911 (2009).
8. Hagn, F., Eisoldt, L., Hardy, J. G., Vendrely, C., Coles, M., Scheibel, T. & Kessler, H. A conserved spider silk domain acts as a molecular switch that controls fibre assembly. *Nature* **465,** 239–242 (2010).
9. Hagn, F. A structural view on spider silk proteins and their role in fiber assembly. *Journal of Peptide Science* **18,** 357365 (2012).
10. Silvers, R., Buhr, F. & Schwalbe, H. The Molecular Mechanism of Spider-Silk Formation. *Angewandte Chemie International Edition* **49,** 54105412 (2010).
11. Kojic, N., Bico, J., Clasen, C. & McKinley, G. H. Ex vivo rheology of spider silk. *Journal of Experimental Biology* **209,** 4355–4362 (2006).
12. Holland, C., Terry, A. E., Porter, D. & Vollrath, F. Comparing the rheology of native spider and silkworm spinning dope. *Nature Materials* **5,** 870–874 (2006).
13. Vollrath, F. & Knight, D. P. Liquid crystalline spinning of spider silk. *Nature* **410,** 541–548 (2001).
14. Jin, H.-J. & Kaplan, D. L. Mechanism of silk processing in insects and spiders. *Nature* **424,** 1057–1061 (2003).
15. Rammensee, S., Slotta, U., Scheibel, T. & Bausch, A. R. Assembly mechanism of recombinant spider silk proteins. *Proceedings of the National Academy of Sciences* **105,** 6590–6595 (2008).
16. Jenkins, J. E., Holland, G. P. & Yarger, J. L. High resolution magic angle spinning NMR investigation of silk protein structure within major ampullate glands of orb weaving spiders. *Soft Matter* **8,** 1947–1954 (2012).
17. Knight, D. P. & Vollrath, F. Liquid crystals and flow elongation in a spider's silk production line. *Proceedings of the Royal Society of London. Series B: Biological Sciences* **266,** 519–523 (1999).
18. Kojic, N., Kojic, M., Gudlavalleti, S. & McKinley, G. Solvent Removal during Synthetic and Nephila Fiber Spinning. *Biomacromolecules* **5,** 1698–1707 (2004).
19. Breslauer, D. N., Lee, L. P. & Muller, S. J. Simulation of Flow in the Silk Gland. *Biomacromolecules* **10,** 49–57 (2009).
20. Lefvre, T., Paquet-Mercier, F., Rioux-Dub, J.-F. & Pzolet, M. Structure of silk by raman spectromicroscopy: From the spinning glands to the fibers. *Biopolymers* **97,** 322336 (2012).
21. Tillinghast, E., Chase, S. & Townley, M. Water extraction by the major ampullate duct during silk formation in the spider, Argiope aurantia Lucas. *Journal of Insect Physiology* **30,** 591–596 (1984).

22. Knight, D. & Vollrath, F. Changes in element composition along the spinning duct in a Nephila spider. *Naturwissenschaften* **88,** 179–182 (2001).

23. Eisoldt, L., Hardy, J. G., Heim, M. & Scheibel, T. R. The role of salt and shear on the storage and assembly of spider silk proteins. *Journal of Structural Biology* **170,** 413–419 (2010).

24. Chen, X., Knight, D. P., Shao, Z. & Vollrath, F. Conformation Transition in Silk Protein Films Monitored by Time-Resolved Fourier Transform Infrared Spectroscopy: Effect of Potassium Ions on Nephila Spidroin Films. *Biochemistry* **41,** 14944–14950 (2002).

25. Boulet-Audet, M., Terry, A. E., Vollrath, F. & Holland, C. Silk protein aggregation kinetics revealed by Rheo-IR. *Acta biomaterialia* **10,** 776–784 (2014).

26. Rey, A. D. & Herrera-Valencia, E. E. Liquid crystal models of biological materials and silk spinning. *Biopolymers* **97,** 374396 (2012).

27. Holland, C., Terry, A., Porter, D. & Vollrath, F. Natural and unnatural silks. *Polymer* **48,** 3388–3392 (2007).

28. Porter, D. & Vollrath, F. Water mediated proton hopping empowers proteins. *Soft Matter* (2012).

29. Moriya, M., Ohgo, K., Masubuchi, Y. & Asakura, T. Flow analysis of aqueous solution of silk fibroin in the spinneret of Bombyx mori silkworm by combination of viscosity measurement and finite element method calculation. *Polymer* **49,** 952–956 (2008).

30. Moriya, M., Roschzttardtz, F., Nakahara, Y., Saito, H., Masubuchi, Y. & Asakura, T. Rheological Properties of Native Silk Fibroins from Domestic and Wild Silkworms, and Flow Analysis in Each Spinneret by a Finite Element Method. *Biomacromolecules* **10,** 929–935 (2009).

31. Plimpton, S. Fast parallel algorithms for short-range molecular dynamics. *Journal of computational physics* **117,** 1–19 (1995).

32. Vollrath, F., Porter, D. & Holland, C. There are many more lessons still to be learned from spider silks. *Soft Matter* **7,** 9595–9600 (2011).

33. Schor, M. & Bolhuis, P. G. The self-assembly mechanism of fibril-forming silk-based block copolymers. *Physical Chemistry Chemical Physics* **13,** 10457–10467 (2011).

34. Schor, M., Martens, A. A., deWolf, F. A., Stuart, M. A. C. & Bolhuis, P. G. Prediction of solvent dependent -roll formation of a self-assembling silk-like protein domain. *Soft Matter* **5,** 2658–2665 (2009).

35. Schor, M., Ensing, B. & Bolhuis, P. G. A simple coarse-grained model for self-assembling silk-like protein fibers. *Faraday Discussions* **144,** 127–141 (2009).

36. Li, M. *Theory and modelling of electrolytes and chain molecules* PhD thesis (The University of Manchester, 2011).

37. Soto-Figueroa, C., del Rosario Rodriguez-Hidalgo, M. & Vicente, L. Dissipative particle dynamics simulation of the micellization–demicellization process and micellar shuttle of a diblock copolymer in a biphasic system (water/ionic-liquid). *Soft Matter* **8,** 1871–1877 (2012).

38. Tang, L., Tjong, V., Li, N., Yingling, Y. G., Chilkoti, A. & Zauscher, S. Enzymatic Polymerization of High Molecular Weight DNA Amphiphiles That Self-Assemble into Star-Like Micelles. *Advanced Materials* (2014).

39. Li, Z. & Dormidontova, E. E. Kinetics of Diblock Copolymer Micellization by Dissipative Particle Dynamics. *Macromolecules* **43,** 3521–3531 (2010).

40. Espanol, P. & Revenga, M. Smoothed dissipative particle dynamics. *Phys. Rev. E* **67,** 026705 (2003).

41. Hu, X. Y. & Adams, N. A. Angular-momentum conservative smoothed particle dynamics for incompressible viscous flows. *Physics of Fluids* **18,** 101702 (2006).

42. Vázquez-Quesada, A., Ellero, M. & Español, P. Consistent scaling of thermal fluctuations in smoothed dissipative particle dynamics. *The Journal of chemical physics* **130,** 034901 (2009).

43. Monaghan, J. J. Smoothed particle hydrodynamics. *Reports On Progress in Physics* **68,** 1703–1759 (2005).

44. Litvinov, S., Ellero, M., Hu, X. & Adams, N. Self-diffusion coefficient in smoothed dissipative particle dynamics. *The Journal of chemical physics* **130,** 021101 (2009).

45. Bian, X., Litvinov, S., Qian, R., Ellero, M. & Adams, N. A. Multiscale modeling of particle in suspension with smoothed dissipative particle dynamics. *Physics of Fluids* **24,** 012002 (2012).

46. Litvinov, S., Ellero, M., Hu, X. & Adams, N. Particle-layering effect in wall-bounded dissipative particle dynamics. *Physical Review E* **82,** 066704 (2010).

47. Litvinov, S., Ellero, M., Hu, X. & Adams, N. Smoothed dissipative particle dynamics model for polymer molecules in suspension. *Physical Review E* **77,** 066703 (2008).

48. Bouchoux, A., Schorr, D., Daff, A., Cambert, M., Gsan-Guiziou, G. & Mariette, F. Molecular Mobility in Dense Protein Systems: An Investigation through 1H NMR Relaxometry and Diffusometry. *The Journal of Physical Chemistry B* **116,** 11744–11753 (2012).

49. Vishnyakov, A., Talaga, D. S. & Neimark, A. V. DPD Simulation of Protein Conformations: From -Helices to -Structures. *The Journal of Physical Chemistry Letters,* 3081–3087 (2012).

50. Groot, R. D. Electrostatic interactions in dissipative particle dynamicssimulation of polyelectrolytes and anionic surfactants. *The Journal of Chemical Physics* **118,** 11265–11277 (2003).

51. Litvinov, S., Hu, X., Ellero, M. & Adams, N. Mesoscopic simulation of the transient behavior of semi-diluted polymer solution in a microchannel following extensional flow. *Microfluidics and Nanofluidics* **16,** 257–264 (2014).

52. Litvinov, S., Hu, X. & Adams, N. Numerical simulation of tethered DNA in shear flow. *Journal of Physics: Condensed Matter* **23,** 184118 (2011).

53. Zhang, Z. & Guo, H. A computer simulation study of the anchoring transitions driven by rodcoil amphiphiles at aqueousliquid crystal interfaces. *Soft Matter* **8,** 5168 (2012).

54. Yan, L.-T. & Xie, X.-M. Computational modeling and simulation of nanoparticle self-assembly in polymeric systems: Structures, properties and external field effects. *Progress in Polymer Science* **38,** 369–405 (2013).

55. He, L., Pan, Z., Zhang, L. & Liang, H. Microphase transitions of block copolymer/nanorod composites under shear flow. *Soft Matter* **7,** 1147–1160 (2011).

56. Vollrath, F. & Porter, D. Spider silk as archetypal protein elastomer. *Soft Matter* **2,** 377–385 (2006).

57. Porter, D., Vollrath, F. & Shao, Z. Predicting the mechanical properties of spider silk as a model nanostructured polymer. *The European Physical Journal E* **16,** 199–206 (2005).

58. Ortlepp, C. S. & Gosline, J. M. Consequences of forced silking. *Biomacromolecules* **5,** 727–731 (2004).

59. Ayoub, N. A., Garb, J. E., Kuelbs, A. & Hayashi, C. Y. Ancient properties of spider silks revealed by the complete gene sequence of the prey-wrapping silk protein (AcSp1). *Molecular biology and evolution* **30,** 589–601 (2013).

60. Davies, G., Knight, D. & Vollrath, F. Structure and function of the major ampullate spinning duct of the golden orb weaver, *Nephila edulis*. *Tissue and Cell* **45,** 306–311 (2013).

61. He, P., Li, X., Deng, M., Chen, T. & Liang, H. Complex micelles from the self-assembly of coil-rod-coil amphiphilic triblock copolymers in selective solvents. *Soft Matter* **6,** 1539–1546 (2010).

62. Zhao, T. & Wang, X. Phase behavior of lyotropic rigid-chain polymer liquid crystal studied by dissipative particle dynamics. *The Journal of chemical physics* **135,** 244901 (2011).